EuroIntervention 2019;15:452-456 published online May 2019

innovation

In vivo intravascular photoacoustic imaging of plaque lipid in coronary atherosclerosis

Sophinese Iskander-Rizk[1], MSc; Min Wu[2], PhD; Geert Springeling[3], BSc; Heleen M.M. van Beusekom[1], PhD; Frits Mastik[1], ND; Maaike te Lintel Hekkert[1], BSc; Robert H.S.H. Beurskens[1], BSc; Ayla Hoogendoorn[1], MSc; Eline M.J. Hartman[1], MD; Antonius F.W. van der Steen[1,4], PhD; Jolanda J. Wentzel[1], PhD; Gijs van Soest[1]*, PhD

1. Department of Cardiology, Erasmus MC University Medical Center Rotterdam, Rotterdam, the Netherlands; 2. Department of Biomedical Engineering, Technical University Eindhoven, Eindhoven, the Netherlands; 3. Department of Experimental Medical Instrumentation, Erasmus MC University Medical Center Rotterdam, Rotterdam, the Netherlands; 4. Department of Imaging Physics, Delft University of Technology, Faculty of Applied Sciences, Delft, the Netherlands

S. Iskander-Rizk and M. Wu contributed equally to this manuscript.

This paper also includes supplementary data published online at: https://eurointervention.pcronline.com/doi/10.4244/EIJ-D-19-00318

KEYWORDS

- intravascular ultrasound
- optical coherence tomography
- other imaging modalities

Abstract

Prospective identification of lipid-rich vulnerable plaque has remained an elusive goal. Intravascular photoacoustics, a hybrid optical and ultrasonic technology, was developed as a tool for lipid-rich plaque imaging. Here, we present the first *in vivo* images of lipid-rich coronary atherosclerosis acquired with this new technology in a large animal model, and relate them to independent catheter-based imaging and histology.

**Corresponding author: Erasmus MC, Thoraxcenter Biomedical Engineering, PO Box 2040, 3000 CA Rotterdam, the Netherlands. E-mail: g.vansoest@erasmusmc.nl*

SUBMITTED ON 29/03/2019 - REVISION RECEIVED ON 1st 17/04/2019 / 2nd 01/05/2019 / 3rd 09/05/2019 - ACCEPTED ON 10/05/2019

DOI: 10.4244/EIJ-D-19-00318

Abbreviations

ACS	acute coronary syndrome
IVOCT	intravascular optical coherence tomography
IVPA	intravascular photoacoustic
IVUS	intravascular ultrasound
LAD	left anterior descending coronary artery
NIRS	near-infrared spectroscopy
PCI	percutaneous coronary intervention
RCA	right coronary artery
TCFA	thin-cap fibroatheroma

Introduction

Lipid-rich atherosclerotic plaques in the coronary circulation cause the majority of acute coronary syndromes (ACS) and cardiac deaths. Plaques that may trigger adverse events frequently have a lipid-rich necrotic core with a thin fibrous cap (thin-cap fibroatheroma [TCFA]), large plaque burden, and a small lumen[1]. Prospective detection of such "vulnerable" plaques, by imaging plaque morphology and composition, may enable pre-emptive interventions. Today's clinically available technology cannot characterise all these features simultaneously[2]. Intravascular optical coherence tomography (IVOCT) has adequate resolution for imaging thin caps, but lipid detection is based on qualitative interpretation. Only intravascular ultrasound (IVUS) quantifies plaque burden. Near-infrared spectroscopy (NIRS) is validated for lipid-core plaque detection but lacks depth resolution.

Intravascular photoacoustic (IVPA) imaging has been proposed for comprehensive characterisation of coronary atherosclerotic plaques. In photoacoustic imaging, one sends a short laser pulse and receives the ultrasound signal generated by optical absorption **(Figure 1)**. Thus, optical absorbers can be localised through the acoustic propagation delay. Plaque lipid has been a prominent IVPA target: by selecting appropriate laser wavelengths, a unique and specific lipid image can be generated. Multimodal IVPA/IVUS data provide a rich combination of structural and composition imaging. The resolution of IVPA is comparable with IVUS. In this study, improved catheter geometry[3] and validation of an animal atherosclerotic model[4] enabled the first IVPA images of coronary atherosclerosis *in vivo*, a crucial step in the clinical translation of this new modality.

Methods and materials

The imaging system[5] consisted of two pulsed lasers with wavelength $\lambda \approx 1{,}725$ nm, ultrasound pulser, signal filtering and data acquisition hardware. A rotary joint (1,200 rpm) coupled the optical and electrical pulses to the IVPA/IVUS catheter (1 mm diameter), comprising an ultrasound transducer (40 MHz) and an optical fibre terminating with an angled mirror[3] **(Supplementary Figure 1)**. IVPA and IVUS signals were digitally filtered to suppress noise and artefacts.

Familial hypercholesterolaemia Bretoncelles Meishan (FBM) mini-swine developed atherosclerosis after nine months of a high-fat diet[4]. The present study, approved by the local animal welfare committee (DEC-EMC3125[109-12-25]), was performed according to the National Institutes of Health Guide for the Care and Use of Laboratory Animals. The right coronary artery (RCA) and the left anterior descending coronary artery (LAD) were imaged using IVPA/IVUS, IVOCT and NIRS/IVUS. IVPA/IVUS pullback (1 mm/s) was performed under manual flushing of the artery with a saline solution from heavy water. All imaging was documented on angiography. After sacrifice, the coronary arteries were dissected from the epicardium, sectioned, and stained with Oil Red O.

Full methods are available in **Supplementary Appendix 1**.

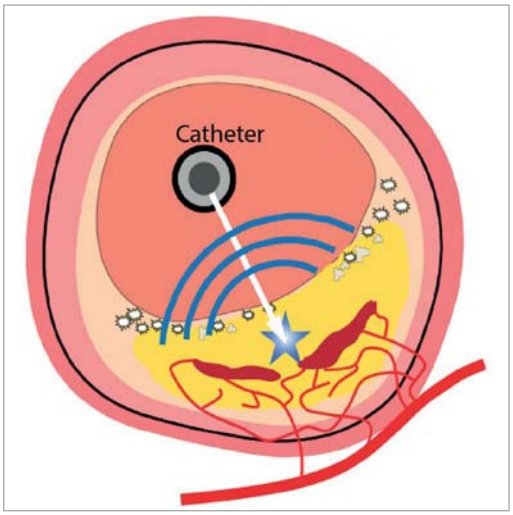

Figure 1. *A hybrid optical/ultrasound catheter illuminates the vessel wall with nanosecond-pulsed infrared light. Chemically specific optical absorption generates ultrasound signals which can be detected, enabling imaging of tissue composition, including lipids.*

Results

The LAD and RCA of an FBM mini pig were successfully imaged with IVPA/IVUS, NIRS/IVUS and IVOCT. NIRS/IVUS did not detect lipid-rich plaque in either artery; however, it revealed intimal thickening in the LAD and a near absence of abnormalities in the RCA. IVOCT confirmed these observations.

IVPA in the LAD distally **(Figure 2)** revealed a circumferential positive signal in the intimal layer **(Figure 2A, Moving image 1)**. The IVPA signal exhibits the familiar "sawtooth" motion pattern of IVUS pullbacks **(Figure 2B)**. This pattern confirms the tissue origins of IVPA signals in all data discussed here, as it is absent in artefactual signals. Circumferential intimal lipids, but no necrotic core, are present in a histological section from the imaged segment **(Figure 2C)**. The intima in IVOCT is heterogeneous, but not strongly attenuating, suggestive of extracellular lipids or foamy macrophages. NIRS confirmed the absence of necrosis **(Figure 2D)**.

In the proximal LAD **(Figure 3)**, the IVPA signal indicates the focal presence of intimal (**Figure 3B**, white arrowheads) and peri-adventitial lipids (blue arrowheads). IVOCT **(Figure 3A)** shows signal-poor areas, consistent with extracellular lipid. Histology **(Figure 3D, Figure 3E)** demonstrates heterogeneously dispersed intimal lipid in this segment. Mild disease was found in the RCA

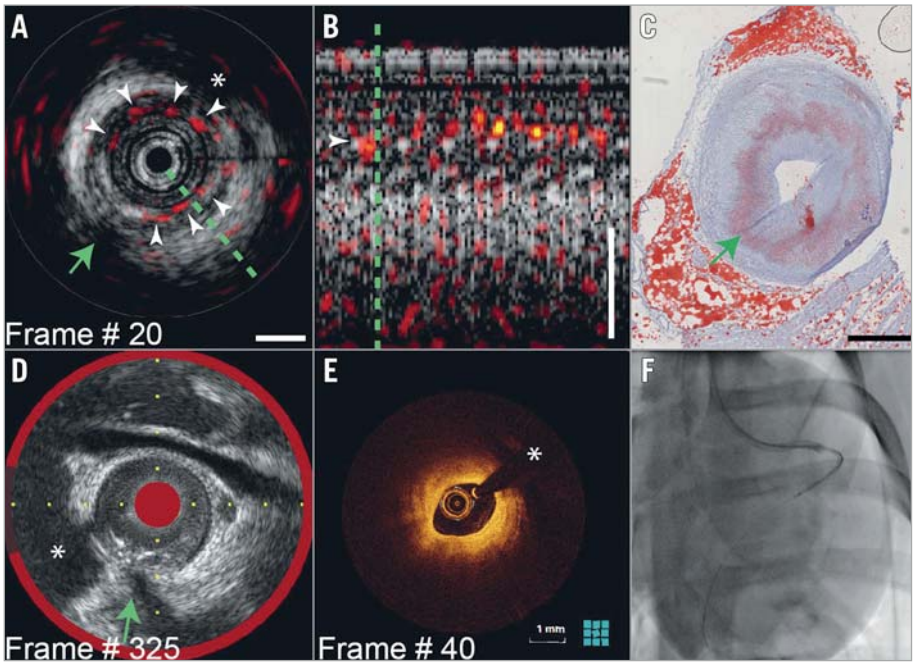

Figure 2. *IVPA in the distal LAD (Moving image 1). A) IVPA images (red-yellow-white, dynamic range 20dB) on IVUS (greyscale, dynamic range 30dB, scalebar 1 mm). Intimal lipids generate IVPA signal (white arrowheads). B) Longitudinal section along the green line in A. C) Corresponding histology confirms presence of intimal lipids. D) Matched NIRS/IVUS shows no lipid core plaque. E) Matched IVOCT. F) Angiogram with radiopaque catheter. Green arrow: side branch ostium. *guidewire artefact.*

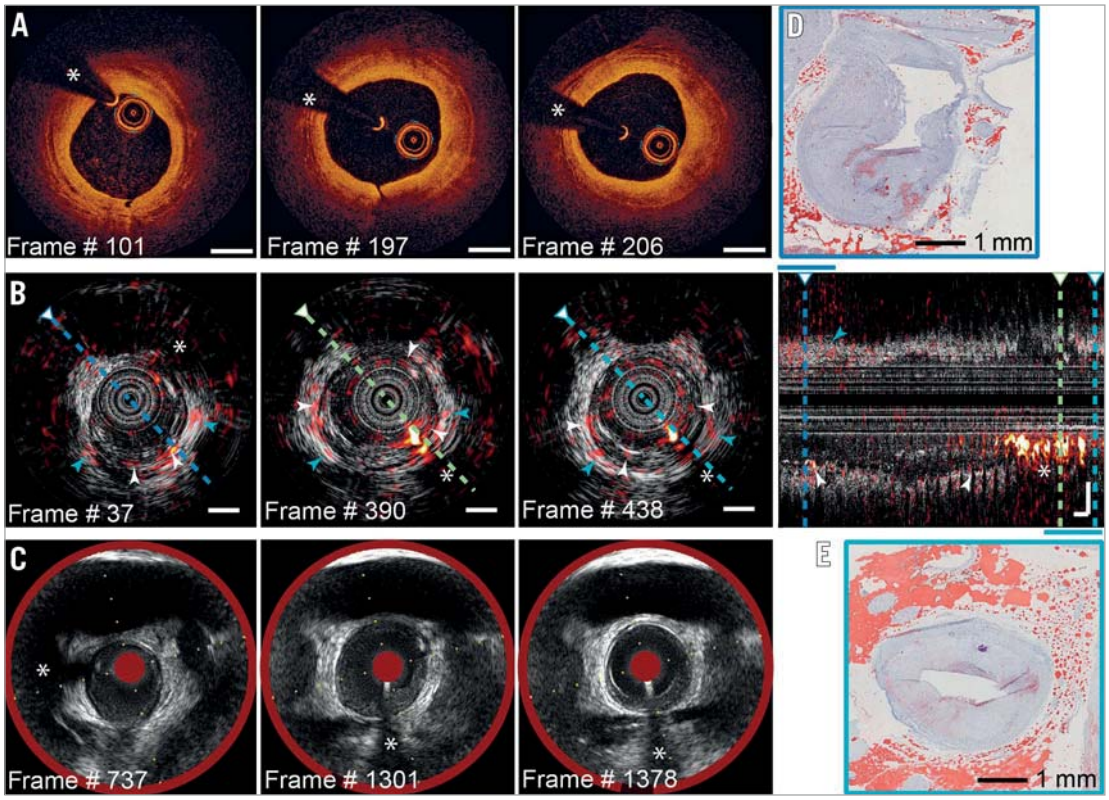

Figure 3. *IVPA/IVUS in the proximal LAD. Selected matched frames: A) IVOCT; B) IVPA/IVUS, with longitudinal section; C) NIRS/IVUS. Histology in the distal (D) and proximal (E) segments confirms focal intimal lipids; cf. (B) (white arrowheads), and perivascular fat (blue arrowheads). Scalebars 1 mm; dynamic range as in Figure 2.*

(Figure 4), according to IVOCT **(Figure 4A)** and IVUS/NIRS **(Figure 4C)**, with perivascular lipids evident on IVPA **(Figure 4B, Supplementary Figure 2, Moving image 2)**.

Discussion and limitations

Lipids exhibit characteristic absorption bands allowing identification and localisation in tissue by photoacoustics. In this study, we demonstrate *in vivo* IVPA imaging of coronary lipid in an atherosclerotic swine. The imaging catheter and operation of the system are similar to IVUS, the difference being the application of saline flush. Further development of the technology (e.g., catheter sheath, noise-suppressing electronics and dual-frequency transducer) and evaluation in clinical trials are needed to establish the utility of IVPA and imaging criteria that may improve outcomes.

Imaging of lipid-rich plaque during PCI may improve our understanding of the risk of developing future ACS, and as such inform treatment strategy. Unlike NIRS, IVPA locates lipids relative to the lumen border, as shown in our data. Multi-wavelength IVPA distinguishes plaque lipid from perivascular fat. Enhanced ultrasonic sensitivity and noise immunity of the system will enable this distinction in future studies and also eliminate the need for flushing. In its present form, IVPA resolution is

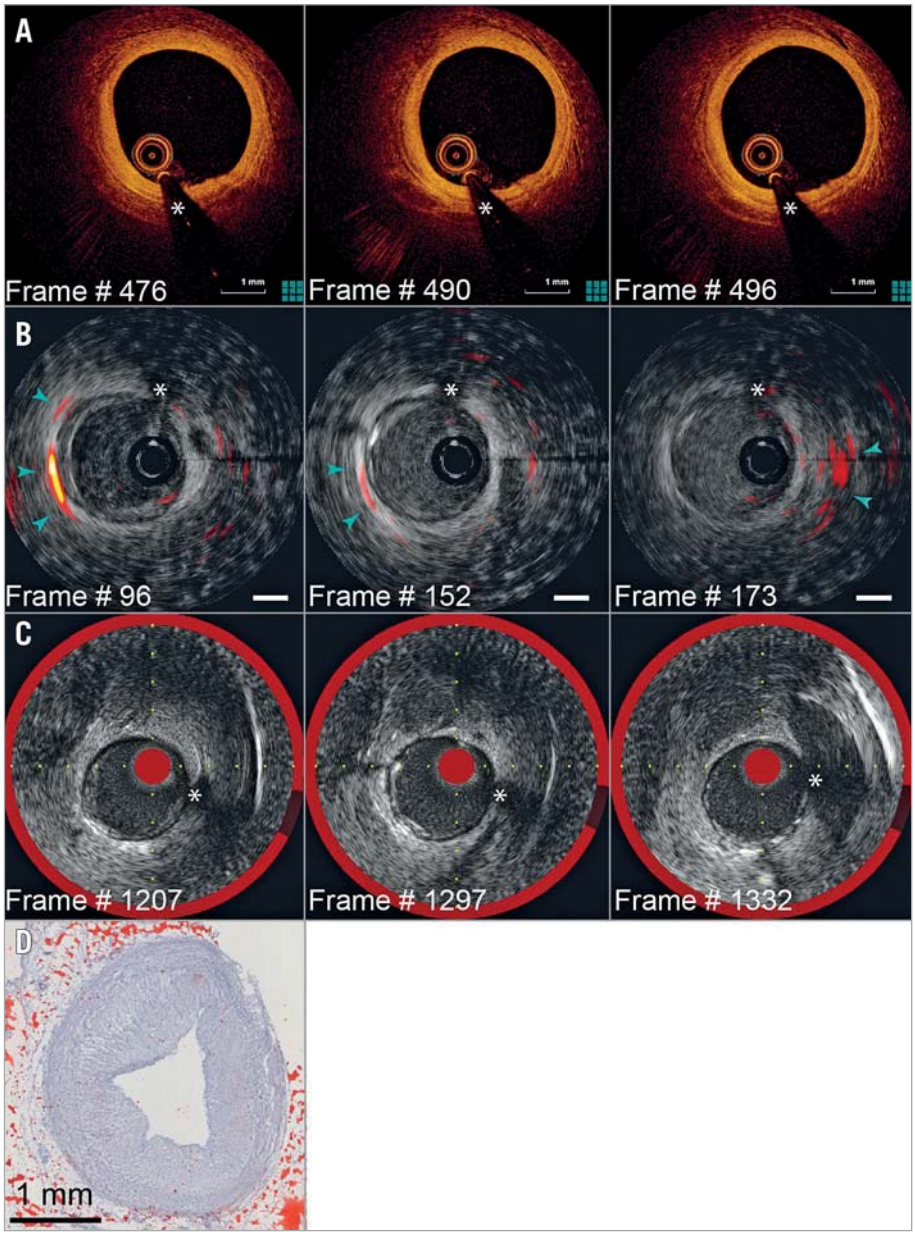

Figure 4. *Pullback imaging in the RCA (Moving image 2, Supplementary Figure 2). Selected matched frames: A) IVOCT; B) IVPA/IVUS; the IVPA signal originates from peri-adventitial lipids (blue arrowheads). C) NIRS/IVUS. D) Histology confirms absence of plaque lipids. Scalebars 1 mm; dynamic range as in Figure 2.*

insufficient to measure cap thickness. One may assess plaque lipid "in contact with the lumen", similar to IVUS-VH TCFA identification[1].

Aspects of this preclinical study limit the scope of the conclusions which can be drawn from the results. We found extensive lipid-rich plaque, but no necrotic core according to histology or NIRS. Studies with IVPA on human autopsy specimens have demonstrated a strong signal from necrotic core plaque. Data were acquired in two vessels only; consequently, there are insufficient data to quantify the diagnostic accuracy of IVPA. Histology colocation was limited by the procedure of matching pullback location, angiography and frozen tissue blocks.

Conclusions

We have demonstrated IVPA imaging of coronary lipid-rich atherosclerotic plaque *in vivo*. In one artery, extensive plaque was found in which IVPA showed a positive signal for intimal lipids. Another artery exhibited mild intimal thickening with sparse or no lipid. Both findings were confirmed by IVOCT imaging and histology. A miniaturised, flexible catheter could be successfully deployed in the coronary circulation of a swine for pullback imaging, a crucial step in the translation of IVPA towards clinical trials.

Impact on daily practice

This study highlights the potential for future clinical translation of a new catheter-based technology for imaging lipid-rich atherosclerotic plaque – intravascular photoacoustics. It detects lipids, but importantly it also locates them in depth in a structural IVUS image. In the future, such data may provide a prospective, lesion-specific risk assessment for adverse cardiac events.

Acknowledgements

We thank Mathijs Stam, from the Department of Experimental Cardiology at Erasmus MC for preparing the histology.

Funding

Netherlands Organization for Scientific Research (NWO) 16131, 12706; European Research Council (310457).

Conflict of interest statement

The authors have no conflicts of interest to declare.

References

1. Stone GW, Maehara A, Lansky AJ, de Bruyne B, Cristea E, Mintz GS, Mehran R, McPherson J, Farhat N, Marso SP, Parise H, Templin B, White R, Zhang Z, Serruys PW; PROSPECT Investigators. A prospective natural-history study of coronary atherosclerosis. *N Engl J Med.* 2011;364:226-35.

2. van Soest G, Marcu L, Bouma BE, Regar E. Intravascular imaging for characterization of coronary atherosclerosis. *Curr Opin Biomed Eng.* 2017;3:1-12.

3. Iskander-Rizk S, Wu M, Springeling G, Mastik F, Beurskens RHSH, van der Steen AFW, van Soest G. Catheter design optimization for practical intravascular photoacoustic imaging (IVPA) of vulnerable plaques. *Proc SPIE.* 2018;10471: 1047111.

4. Thim T, Hagensen MK, Drouet L, Bal Dit Sollier C, Bonneau M, Granada JF, Nielsen LB, Paaske WP, Botker HE, Falk E. Familial hypercholesterolaemic downsized pig with human-like coronary atherosclerosis: a model for preclinical studies. *EuroIntervention.* 2010;6:261-8.

5. Wu M, Springeling G, Lovrak M, Mastik F, Iskander-Rizk S, Wang T, van Beusekom HM, van der Steen AF, Van Soest G. Real-time volumetric lipid imaging in vivo by intravascular photoacoustics at 20 frames per second. *Biomed Opt Express.* 2017;8:943-53.

Supplementary data

Supplementary Appendix 1. Methods and materials.

Supplementary Figure 1. Intravascular photoacoustic imaging system components.

Supplementary Figure 2. Intravascular photoacoustic/ultrasound pullback images in the RCA.

Moving image 1. Stationary scan of IVPA (red-yellow-white, dynamic range 20dB) and IVUS (greyscale, dynamic range 30dB, scalebar 1 mm) in the distal LAD; moving average over three cardiac cycles.

Moving image 2. Pullback recording of IVPA (red-yellow-white, dynamic range 20dB) and IVUS (greyscale, dynamic range 30dB, scalebar 1 mm) in the distal RCA displayed in **Supplementary Figure 2**.

The supplementary data are published online at: https://eurointervention.pcronline.com/doi/10.4244/EIJ-D-19-00318

Supplementary data

Supplementary Appendix 1. Methods and materials

1. Imaging system

The imaging system we used is schematically shown in **Supplementary Figure 1A**; the catheter design is shown in **Supplementary Figure 1B**. Briefly, a delay generator (BNC 575; Berkeley Nucleonics Corporation, San Rafael, CA, USA) triggered two lasers (FQ-OPO; Elforlight Ltd., Daventry, UK), an ultrasound pulser and a digital acquisition card (DAQ) (PX14400; Signatec, New York, NY, USA). Every A-line acquisition was composed of one pulse-echo and two photoacoustic acquisitions at a wavelength $\lambda \approx 1{,}725$ nm. The compound A-line acquisition rate was 5 kHz, limited by the laser pulse repetition frequency. The catheter was rotated at 1,200 rpm, resulting in 20 frames per second of 250 A-lines per frame. The pullback speed was 1 mm/s. The IVPA/IVUS catheter comprised a 40 MHz ultrasound single element transducer (50% bandwidth; Blatek Industries, Inc., State College, PA, USA) and a 200 μm diameter optical fibre, enclosed in a flexible drive shaft (outer diameter 0.8 mm; Asahi Intecc., Aichi, Japan). A silver-coated prism deflected the light at the output of the catheter. The rotating core was fitted into the sheath of a commercially available NIRS/IVUS catheter (TVC Insight Coronary Imaging Catheter; Infraredx, Burlington, MA, USA), which had radiopaque markers. The lasers were coupled to the rotating optical fibre of the IVPA/IVUS catheter through a home-built rotary joint **(Supplementary Figure 1C)**. The laser pulse energy at the output of the catheter ranged between 40 and 50 μJ. Acquired data were amplified (43dB; AU1263; Miteq, Long Island, NY, USA) and band-pass filtered (13-60 MHz 5^{th} order Butterworth; built in-house) before digitisation (14-bit, 400 MHz), processing and visualisation.

2. Animal model and imaging protocol

Invasive imaging of the coronary arteries of a familial hypercholesterolemia Bretoncelles Meishan (FBM) mini-swine was performed. The swine was fed a restricted high-fat diet (10% lard and 0.75% cholesterol; The National Institute of Agronomic Research, France) for 9 months to promote atherosclerotic plaque development. The animal study, approved by the local animal ethics committee (DEC EMC3125 [109-12-25]), was performed according to the National Institutes of Health Guide for the Care and Use of Laboratory Animals. The animal (castrated male, 74 kg) was sedated using a mix of xylazine (2.25 mg/kg, 20 mg/ml) and Zoletil 100 (tiletamine/zolazepam; 6 mg/kg, 100 mg/ml) injected intramuscularly. Anaesthesia was induced by sodium thiopental (4 mg/kg, 50 mg/ml) and

maintained by isofluorane inhalation (1-2.5% v/v). Through a sheath in the carotid artery, 250 mg of acetylsalicylic acid (Aspegic; Sanofi-Aventis Nederlands BV, Gouda, the Netherlands) and 10,000 IU of heparin (Heparine; Leo Pharma, Amsterdam, the Netherlands) were administered intra-arterially, the latter being subsequently injected every hour in a dose of 5,000 IU.

Access to the ostia of the right coronary artery (RCA) and the left anterior descending coronary artery (LAD) was achieved by inserting a guiding catheter (Mach 1, 8 Fr; Boston Scientific, Marlborough, MA, USA) through the carotid sheath. This process, as well as imaging catheter positions (start and end of pullback) in the coronary arteries, was guided by angiography. We imaged the coronary vasculature with three imaging modalities: IVPA/IVUS as described above, commercial IVOCT (ILUMIEN™ Optis™ with Dragonfly™ Optis catheter; St. Jude Medical, St. Paul, MN, USA) and NIRS/IVUS (TVC Insight Coronary Imaging Catheter; Infraredx, Burlington, MA, USA). The IVOCT pullback (36 mm/s) required the artery to be flushed from blood with contrast (Visipaque 320; GE Healthcare, Chicago, IL, USA) under a constant flush rate of 4 ml/s (Medrad Injection System; Bayer HealthCare LLC, Whippany, NJ, USA). Similarly, the IVPA/IVUS pullback (1 mm/s) was performed under manual flushing of the artery from blood with a saline solution based on heavy water (deuterium oxide [D_2O]), an optically clear liquid at the imaging wavelength. After imaging, the animal was sacrificed by an overdose of pentobarbital (Euthasate; AST Farma, Oudewater, the Netherlands).

3. Data processing

Digital processing of the data acquired was performed on MATLAB® (R2017b; MathWorks, Natick, MA, USA). Ultrasound signals were band-pass filtered between 16 and 60 MHz, while photoacoustic signals were band-pass filtered between 14 and 21 MHz (4^{th} order Butterworth). To accommodate for transmit artefacts, tubing artefacts and high-frequency glitches, data were individually corrected for jitter and high-pass filtered across the A-lines to remove repeating signals. The samples representing the space within the catheter inner tube were blacked out. The two IVPA acquisitions in each A-scan were summed to improve signal-to-noise ratio (SNR). A 3D median filter of kernel 3×3×3 voxels was applied to suppress interference noise. Final images were used to assess lipid deposition in the vessel, and compared to histology and independent imaging.

Using angiographic guidance, it was confirmed that the NIRS/IVUS and IVOCT (pullback length of approximately 75 mm) fully covered the IVPA/IVUS pullbacks (length of 20-25 mm). The NIRS/IVUS and IVOCT pullbacks were matched by two independent experts based on angiographic records and anatomic landmarks. IVPA/IVUS was matched to NIRS/IVUS based on angiographic position, side branches, and identifiable features on IVUS images of both modalities.

4. Histology

After imaging and animal sacrifice, the coronary arteries, including the ostium, were dissected from the epicardium, embedded for cryosectioning, and frozen on dry ice. Arteries were stored at -80˚C until further preparation for histology. At four locations (both vessels proximal and distal) we cut three sections separated by 4 mm; we estimated longitudinal vessel shrinking following dissection and freezing at 30%. These were stained with Oil Red O (ORO), which stains lipids in pink/red, and counterstained with haematoxylin.

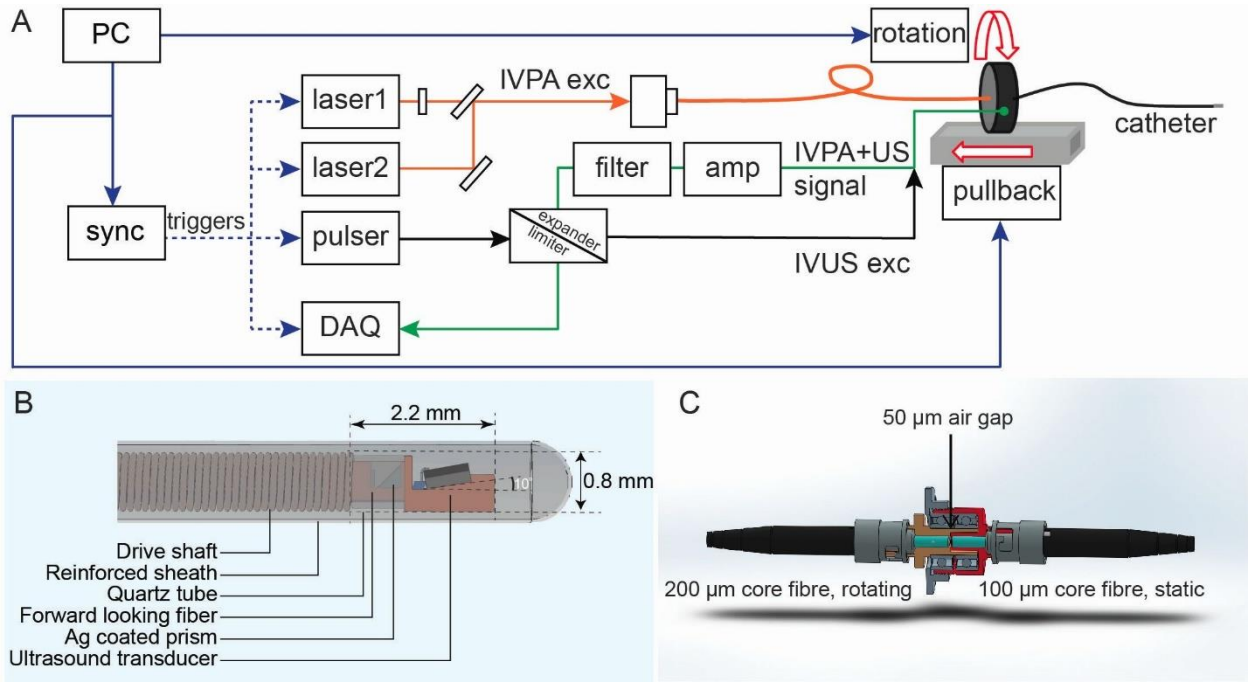

Supplementary Figure 1. Intravascular photoacoustic imaging system components.

A) System diagram. Blue: control and timing, orange: optical signal, black: analogue pulse signal, green: analogue received echo. B) Sketch of the catheter tip. C) Design of the rotary joint.

Ag: silver; amp: amplifier; DAQ: data acquisition; exc: excitation; PC: computer; sync: synchronisation unit

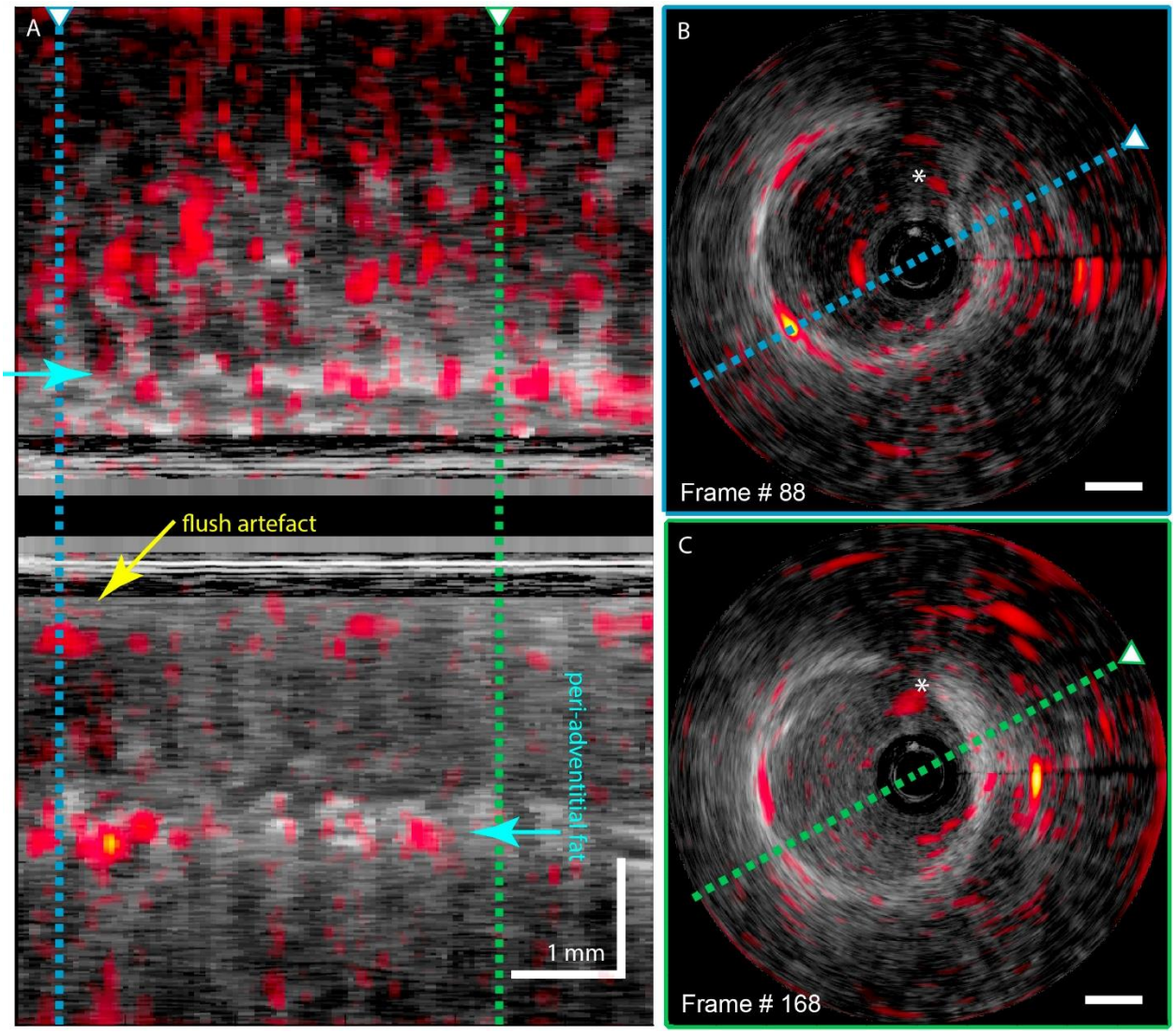

Supplementary Figure 2. Intravascular photoacoustic/ultrasound pullback images in the RCA.

A) Longitudinal section through the IVPA (red-yellow-white, dynamic range 20dB) and IVUS (greyscale, dynamic range 30dB, scalebar 1 mm) at the plane represented by the lines in the cross-sectional images B (at blue line in A) and C (at green line in A). Arrows in panel A indicate peri-adventitial fat, and a positive signal that does not coincide with tissue an artefact attributed to incomplete flush.